



Cite this: *Environ. Sci.: Atmos.*, 2025, 5, 1341

## An optimization of transmission measurement of an atmospheric pressure interface time-of-flight mass spectrometer (APi-ToF MS)

Dina Alfaouri,<sup>a</sup> Monica Passananti,<sup>b</sup> \*<sup>ab</sup> Nina Sarnela,<sup>a</sup> Juha Kangasluoma<sup>a</sup> and Hanna Vehkamäki <sup>a</sup>

Evaluating an instrument's performance is just as important, if not more, than its intended purpose. Mass spectrometers, in particular, have been extensively studied and analyzed due to their key role in many applications across various fields. One type of mass spectrometer, the atmospheric pressure interface time-of-flight mass spectrometer (APi-ToF MS), is widely used for measuring reactive trace gases and aerosol precursors. This study investigates the transmission efficiency of an APi-ToF MS coupled with two distinct ionization sources: an electrospray ionizer (ESI) and a nickel–chromium wire generator. Each ion source was integrated into a separate experimental setup, with the ESI paired with a planar differential mobility analyzer (P-DMA) and the wire generator combined with a Half-mini differential mobility analyzer (Half-mini DMA). The transmission efficiency was quantified by calculating the ratio of ions entering the mass analyzer to those detected at the end detector. The primary aim of this study is twofold: (1) to develop and validate a standardized procedure for quantifying transmission efficiency in APi-ToF MS systems, and (2) to critically evaluate an alternative measurement approach using a distinct ionization–mobility setup. We propose an optimized protocol for assessing transmission efficiency, providing a framework that future researchers can adapt to characterize their own instruments. Our results reveal different transmission trends between negative and positive samples, and compares the different methods explored in this study with each other and with previous studies. The ESI–P-DMA–APi-ToF MS setup was shown based on our results to be significantly more accurate, mainly since the errors on the mass/charge axis are remarkably lower, than the wire generator–Half-mini DMA–APi-ToF MS setup in determining the transmission efficiencies.

Received 24th February 2025  
Accepted 15th October 2025

DOI: 10.1039/d5ea00029g

rsc.li/esatmospheres

### Environmental significance

To understand atmospheric processes at chemical level the use of mass spectrometry (MS) is crucial. It allows for the identification and quantification of molecules and clusters present in the atmosphere. However, to obtain reliable data the MS instrument needs to be characterized. For example, a correct ion transmission measurement is needed to convert the ion signals from the MS into concentration. We describe two methods to measure the transmission of an Atmospheric Pressure interface Time of Flight (APi-ToF) MS, widely used in atmospheric science research, and we highlight pros and cons. We suggest a procedure to simplify the transmission measurement and increasing its accuracy. Implementing these measurements for characterizing an APi-ToF-MS will significantly improve the quality of the data collected.

## 1. Introduction

High-resolution mass spectrometers have been in recent years developed and widely adopted across various fields, including atmospheric science. This experimental analytical tool provides indispensable insights into the chemical composition of the studied samples.<sup>1,2</sup> However, it is crucial to rigorously examine and evaluate the performance of these instruments, by

assessing transmission and overall functionality to ensure accurate representation of sample constituents and enable reliable data analysis.<sup>3–5</sup> The transmission is a crucial parameter for the quantification of the analytes; indeed, the relative intensity of the detected compounds depends not only on their relative concentrations in the sample, but also on the charging efficiency and on the transmission. Atmospheric Pressure Interface Time-of-Flight Mass Spectrometers (APi-ToF MS) are a specific type of mass spectrometer employed in atmospheric applications. Previous studies<sup>4,6</sup> have taken a deep look into the performance of high-resolution mass spectrometers, specifically APi-ToF MS. The instrument's transmission, which is

<sup>a</sup>Institute for Atmospheric and Earth System Research / Physics, Faculty of Science, University of Helsinki, Finland. E-mail: monica.passananti@helsinki.fi

<sup>b</sup>Dipartimento di Chimica, Università di Torino, Via Pietro Giuria 5, 10125 Turin, Italy



defined as the ratio of the detected ions and the ions entering the inlet,<sup>7</sup> is a critical parameter to assess. The transmission depends mainly on the geometry, the pressures and the voltage configuration. The latter is defined as the combination of the voltages applied both to the API and the ToF and play a key role in the transmission. Indeed, loss of charged ions inside the instrument is mass dependent and strongly affected by the voltage configurations.<sup>7</sup> Mass discrimination effects occur in different parts of the API-ToF MS, particularly in the API interface (the two quadrupole units), the ToF's orthogonal extraction unit, and the multi-channel plate detector (MCP).<sup>6</sup> All the losses of charged ions across these different parts contribute largely to the relatively low transmission of the instrument.

API-ToF's are used in atmospheric sciences with different chemical ionization chemistries in order to measure vast amount of different reactive trace gases and aerosol precursors.<sup>8,9</sup> The calibration for the concentration measurement of reactive gases or condensable vapors is challenging as the compounds will undergo chemical reactions or be lost in the walls of the calibration system, and this will cause large uncertainties in the measurements. The measurements of condensable vapors rely strongly on calibration with sulfuric acid<sup>10</sup> where the sulfuric acid is produced from sulfur dioxide *in situ*. When calculating the concentrations of other condensable vapors such as highly oxygenated organic molecules, they are approximated to be charged at collision efficiency<sup>11</sup> and the sulfuric acid calibration factor is used also for them. If the transmission in the mass range of target ions is different from that for the reagent ions that are used for normalizing, it can cause error to the concentrations. In Ehn *et al.* (2014) this difference was approximated to be of a factor 2 at maximum.<sup>11</sup>

Calibration in mass spectrometric measurements of atmospheric species is inherently challenging due to mass-dependent transmission biases intrinsic to the instrument design. Although sulfuric acid is commonly employed as a calibration standard, its relatively low mass/charge fails to adequately represent the transmission efficiency of higher mass/charge species, such as highly oxidized organic molecules and atmospheric clusters. These heavier species often experience disproportionately greater transmission losses. Contributing factors include instrument specific parameters such as quadrupole RF voltages, and pressure differentials across the ion optics impose mass/charge selective transmission characteristics.<sup>6</sup> Relying on a single calibrant like sulfuric acid is therefore not representative of the wide chemical and physical diversity of ambient ions and clusters typically encountered in the atmosphere. It does not substitute for a proper transmission efficiency characterization. Given the compositional complexity of ambient measurements and the current lack of widespread use of alternative or complementary calibrants, there is a critical need for systematic transmission evaluations across the full relevant  $m/z$  range. This is essential for achieving quantitative accuracy and improving comparability across instruments and field campaigns.

Transmission efficiency is evaluated by generating ions, selectively separating them, and quantifying their presence before entering the API interface using an electrometer, and at

the end detector of the API-ToF MS. Subsequently, comparison is made between the ion counts registered by the API-ToF MS and the electrometer signal. This experimental configuration typically includes an ion source to generate ions; a differential mobility analyzer (DMA), in our case planar or Half-mini type to separate the ions; an electrometer used to detect and quantify the ions before entering the API-ToF; and the API-ToF mass spectrometer itself. Varying the ion source and DMA type allows the evaluation of their impact on the accuracy of the transmission measurements, which has not been investigated previously. Our primary focus is on varying the ion source, with brief consideration given to the effect of the DMA type.

Wire generators consists of a metal wire which produces charged clusters and nanoparticles when heated, depending on the experimental conditions. The main factors influencing the emissions from the wire generator are the surrounding atmosphere (*e.g.* Ar, N<sub>2</sub>, air, *etc.*) and the wires composition. These wires are often used in calibrating and characterizing CPCs (Condensation Particle Counters); and they have also been employed for transmission evaluation of mass spectrometers due to their stable ion production across a broad mass/charge range, as well as possibility of operation in both charging modes (positive and negative).<sup>12,13</sup> Some studies<sup>4,6</sup> have explored also the use of ionic liquids for transmission measurements. In positive mode, the cations of the ionic liquids are usually only considered, whereas in negative mode either the bromide or iodide single ions, or their respective adduct ions (*e.g.*, dimers, trimers), are considered and those may fragment inside the instrument. In both modes, however, their mass/charge coverage was limited (even more so in negative mode), with insufficient data point density within the measured  $m/z$  range. Additionally, in negative mode, the analysis of iodide-adduct dimers and trimers used in determining transmission efficiency did not account for potential fragmentation that could affect the results. Moreover, the method presented in Junninen *et al.*, 2010,<sup>4</sup> relied on positive compounds having only one mass on negative spectrum while large number of atmospheric measurements of condensable vapors and secondary organic aerosol precursors are performed with negative polarity of the mass spectrometer. The other previously introduced method for transmission measurement is based on depleting perfluorinated acids.<sup>6</sup> These acids are detected with negative polarity and have a suitable mass range, but the challenge of the method is caused by with the stickiness of the used compounds that can easily contaminate the whole instrument and cause long memory effects. This contamination can cause serious problems when the instrument is used to detect and quantify molecules at a concentration below one part per trillion (ppt).<sup>14</sup> The depletion method also gives only relative transmission efficiencies.

To overcome these limitations, we employed two complementary ionization techniques: electrospray ionization (ESI), which consistently generates ions suitable for controlled transmission measurements, and a wire generator (with Am-charger), which simulates gas-phase ionization processes similar to some ambient sampling conditions. This dual-method strategy enables a comprehensive evaluation of



transmission efficiency while addressing both calibration accuracy and field-relevant applicability.

In this study, we incorporate an ElectroSpray Ionizer (ESI) coupled with a Planar Differential Mobility Analyzer (P-DMA) into an API-ToF MS setup [Fig. 1(a)], as described in our previous publication.<sup>15</sup> This integrated system is utilized to examine ion transmission within the API-ToF MS, with a comparison to the conventional wire generator method, which comprises a wire generator connected to a Half-mini DMA<sup>16,17</sup> linked to the API-ToF MS [Fig. 1(b)]. The primary objective is to identify suitable samples and procedures that facilitate straightforward transmission measurements using the ESI source (also used for environmental analysis).<sup>18</sup>

The transmission of ions inside a mass spectrometer depends on several factors, and it is strongly affected by the conditions in the regions that guide the ions from the ionization source to the ToF.<sup>4,6,11</sup> Therefore, each instrument will have

a specific transmission curve valid in the conditions (mainly the voltage configuration) used during the transmission experiments; to calculate the transmission of the instrument based only on physics principles requires a complex model and to the best of our knowledge there are no such models developed that are able to quantify the transmission inside the whole API-ToF. Thus, the goal of this work is to define a procedure to measure experimentally the transmission of an API-ToF and highlight the possible source of errors in the experiments and data analysis.

## 2. Materials and methodology

### 2.1 Chemicals

Nine ionic liquids were used in this work. Five of these, tetraethylammonium bromide (>98%), tetraheptylammonium bromide (>99%), hexadecyltrimethylammonium bromide

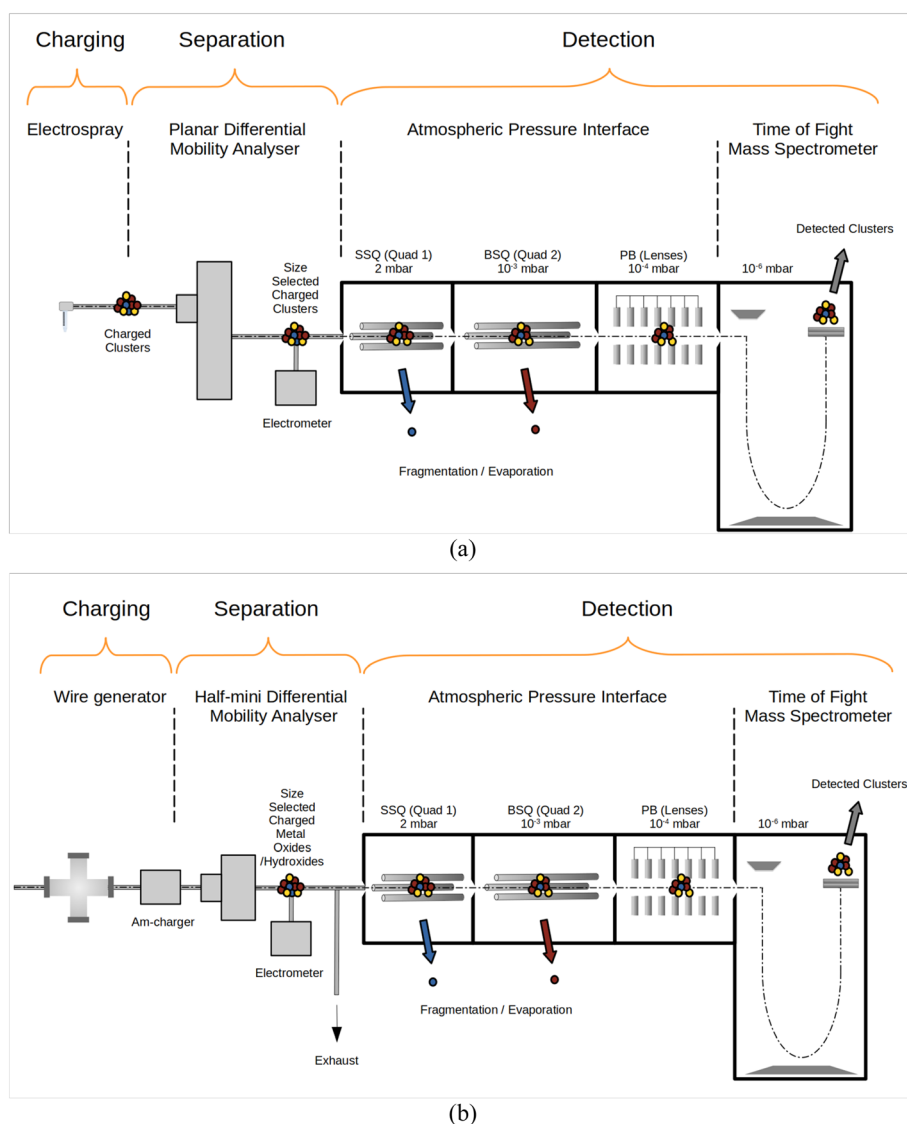


Fig. 1 Illustrations of the experimental set-ups used in this study, adapted and revised from figure in Passananti *et al.* 2019.<sup>7</sup> Setup (a) is an ElectroSpray Ionizer (ESI) coupled with a Planar Differential Mobility Analyzer (P-DMA) connected to the API-ToF MS, and setup (b) is a wire generator connected to a Half-mini DMA linked to the API-ToF MS. Figures are not to scale.



(>98%), and tetraoctadecylammonium bromide (98%), tetrahexyldecylammonium bromide (98%) and methanol, were purchased from Sigma-Aldrich. The remaining four, tetramethylammonium iodide (>99%), tetrapropylammonium iodide (>98%), tetrabutylammonium bromide (>98%), and tetradodecylammonium bromide (>99%), were obtained from Fluka. All reagents were used as received, without further purification. Water used was of Milli-Q quality.

Ionic liquids are salts at liquid state and when ionized by ESI the cation and anion are separated. Beside the monomers (the cations if the analysis is carried in positive mode and the anions if the analysis is carried in negative mode), the sample also contains clusters of these salts composed of two cations and one anion (in positive mode analysis) or two anions and one cation (in negative mode analysis).

In addition to the ionic liquids mixture, a 'Thermo Scientific Pierce ESI Negative Calibration Solution', purchased from Thermo Fisher, was used for the negative mode transmission measurements. This solution contains sodium dodecyl sulfate ( $2.9 \mu\text{g mL}^{-1}$ ), sodium taurocholate ( $5.4 \mu\text{g mL}^{-1}$ ), and Ultramark 1621 (0.001%) in an aqueous solvent composed of 50% acetonitrile, 25% methanol, and 1% acetic acid. It is commonly used for negative mode calibration of certain mass spectrometers, including the Orbitrap.

## 2.2 Setup 1: ESI-P-DMA-API-ToF MS

In this study, the ESI-P-DMA-API-ToF MS was configured for both positive and negative ionization modes. The ESI-P-DMA was produced by SEADM S. L. (Valladolid, Spain),<sup>19</sup> the API-ToF MS is produced by ToFwerk AG (Thun, Switzerland).<sup>4</sup> The ESI utilized a sharpened fused silica emitter with an inner diameter (ID) of  $75 \mu\text{m}$ , an outer diameter (OD) of  $360 \mu\text{m}$ , a length of  $30 \text{ cm}$ , and a  $15^\circ$  sharp tip (The Sharp Singularity™ – Sharpened fused silica emitters, from Fossil Ion Technology S. L.). The P-DMA achieves a resolving power of  $\sim 110$  and is capable of measuring clusters up to  $4 \text{ nm}$  in size.<sup>19</sup> The ESI voltage is varied from  $\pm(2370\text{--}2990) \text{ V}$  to obtain a current of  $\sim 10\text{--}80 \text{ nA}$  at the DMA entrance; capillary flow pressure is set to about  $4.0 \text{ kPa}$ , and kept constant for all the measurements. The DMA was operated in counter flow mode:  $\sim 2 \text{ L per min N}_2$  was supplied to the sheath flow loop, and  $\sim 0.2 \text{ L min}^{-1}$  exited the DMA inlet. The P-DMA voltage ranges and step increments were tailored to the specific sample requirements (parameters reported below). The DMA was initially used to scan through a pre-selected voltage range at fixed voltage increments. Subsequently, it was shifted to fixed voltage scans at pre-determined voltages corresponding to the regions where the desired charged molecules appeared to isolate specific ions.

The inlet flow rate of the API-ToF MS was  $0.8 \text{ L min}^{-1}$  and that of the electrometer  $1 \text{ L min}^{-1}$ . The electrometers used was SEADM LYNX E11. The API-ToF MS consists of an Atmospheric Pressure interface (API), made by three vacuum chambers, coupled with a time-of-flight mass spectrometer.<sup>4</sup> Data were analyzed by ToFTools MatLab toolbox and an in-house software, called FlatDMA-analyser.<sup>20</sup>

Both positive and negative ions were generated and analyzed using this setup, with samples carefully selected to ensure comprehensive coverage of the mass/charge ratio ( $m/z$ ) range from few Th to approximately  $1500 \text{ Th}$ . In both ionization modes, a mixture of nine ionic liquids dissolved in a water/methanol solution was used as the primary sample. Additionally, the 'Thermo Scientific Pierce ESI Negative Calibration Solution' was employed for negative mode measurements. The voltage settings for the API-ToF MS, in both modes, were selected for improving the transmission in the low and medium  $m/z$  range, since this is often the target for atmospheric analysis. In particular, the voltage settings were based on optimized values from Passananti *et al.*, 2019.<sup>7</sup>

In positive mode, the P-DMA was configured to scan a voltage range of  $1000\text{--}8500 \text{ V}$  with a step size of  $15 \text{ V}$ . In negative mode, the voltage scan parameters varied based on the sample: for the ionic liquids mixture, the P-DMA was scanned from  $-1500$  to  $-5500 \text{ V}$  with a step size of  $15 \text{ V}$ , while for the Thermo Fisher sample, it was scanned from  $-2900$  to  $-8500 \text{ V}$  with a step size of  $5 \text{ V}$ . All voltage ranges were optimized to effectively capture the target ionic species.

## 2.3 Setup 2: wire generator-Half-mini DMA-API-ToF MS

The wire generator-Half-mini DMA-API-ToF MS system was configured exclusively in negative ionization mode. The Half-mini DMA, with a resolving power of  $\sim 25\text{--}60$  and a measurable size range of  $1\text{--}30 \text{ nm}$ ,<sup>17</sup> was operated within a voltage range of  $-40$  to  $-300 \text{ V}$  using a step size of about  $1.3 \text{ V}$ . This configuration was chosen to optimize the resolution and sensitivity for the detection of negatively charged particles. The wire generator consists of a metal wire that produces charged clusters and nanoparticles when heated. In our experiments a nickel-chromium wire was employed as the core material for the wire generator, operated under a continuous flow of compressed air to generate ions. An Am-charger was integrated into the system to enhance the charging efficiency of the generated metal oxide particles. This setup ensured consistent ion generation and reliable detection in the negative ionization mode.

A compressed air flow of  $30 \text{ L min}^{-1}$  was supplied to the wire generator, with  $15 \text{ L min}^{-1}$  directed through the Am-charger and subsequently into the Half-mini DMA. A flow rate of  $5 \text{ L min}^{-1}$  was diverted to the TSI electrometer for initial signal measurement, while  $0.8 \text{ L min}^{-1}$  served as the inlet flow for the API-ToF MS. The remaining airflow was discharged to the exhaust.

## 2.4 Transmission calculations

To calculate the transmission efficiency, the first step involved averaging the signal of the electrometer obtained at each fixed voltage scan of the Differential Mobility Analyzer (DMA). Ideally, a single value should be recorded for the output signal at a given voltage; however, minor fluctuations in the signal are expected. Therefore, an averaging step was necessary to ensure consistency. The averaged signal was then converted into a relative output concentration (numbers of ions per  $\text{cm}^3$ ,  $\# \text{ cm}^{-3}$ ).



The second step required obtaining a comparable output signal for the ions detected by the mass spectrometer. The MS data from fixed voltage scans were processed by extracting the output signal as a time series over the measurement period. This signal was then averaged for the ion of interest and converted into a relative concentration ( $\# \text{ cm}^{-3}$ ). It is important to note that when converting both signals into a concentration ( $\# \text{ cm}^{-3}$ ) the signals are normalized against the corresponding flow rates used. Finally, the transmission is subsequently calculated and plotted across the measured mass/charge range.

### 3. Results & discussion

#### 3.1 Setup 1: transmission measurements with electrospray and planar DMA

**3.1.1 Positive mode.** The transmission of the API-ToF MS in positive mode was measured using ionic liquids, due to their easy ionization and high variation in the mass/charge range. We conducted a detailed analysis focusing on the monomer peaks of the nine ionic liquids present in the sample. Monomer peaks were the primary focus due to their importance in achieving as accurate transmission measurements as possible. However, dimer peaks were also observed, though with significantly lower intensity compared to the monomers, given the instrumental settings utilized in this study. Fig. 2 illustrates the full mass spectrum acquired from the sample, highlighting the numbered peaks that correspond to the list of ions provided in the accompanying table. The spectrum reveals an extensive mass/charge ratio ( $m/z$ ) coverage, ranging from 74.17 to 1027.16 Th, with the peaks distributed across this range, ensuring comprehensive representation of the target mass range.

The majority of the selected peaks were intense and much stronger compared to other peaks (dimers and impurities) detected during the measurements, indicating their reliability as standards for transmission measurements. This is further

supported by the mass spectra from the fixed voltage scans, which were highly clean and showed only the peak of the selected ionic liquid monomer. However, in a few cases, specifically for peaks 7, 8, and 9 (see Fig. S1 in the SI), the mass spectra showed multiple monomer peaks simultaneously. The transmission was calculated both including and excluding these peaks and we observed that the transmission trend remained largely unaffected by the presence of these peaks. This is attributed to a combination of factors; in this particular case, the lower intensity of these peaks compared to the peak of interest and the very low transmission efficiency at these higher masses.

The electrometer installed at the entrance of the API-ToF MS allowed us to directly compare the number of ions at the API's inlet with the number of ions that reaches the ToF detector, and evaluate the signal loss between the instrument's inlet and the ToF's end detector (Fig. S2 in the SI shows the signal of the electrometer). This configuration allows us to avoid corrections due to different ion losses from the exit of the DMA, the entrance of the electrometer, and the API-ToF MS, respectively. Thus, this comparison facilitated the calculation of the transmission efficiency of the instrument across the covered mass range. Fig. 3 depicts the transmission percentage as a function of the mass/charge ratio ( $m/z$ ). The transmission efficiency was observed to peak at approximately 0.48% for intermediate mass ranges, while it declined significantly for both lower and higher masses, showcasing the instrument's expected limitations in these regions, with the used voltage configuration of the MS. The measured transmission is around one order of magnitude below the maximum transmission efficiency of our instrument which is  $\sim 4\%$ , considering the extraction frequency is 14 kHz with a 3000 ns pulse width. Junninen *et al.*, 2010,<sup>4</sup> report a similar trend for their positive mode transmission measurements and their corresponding peak transmission efficiency value was between 0.4 and 0.5% as well.

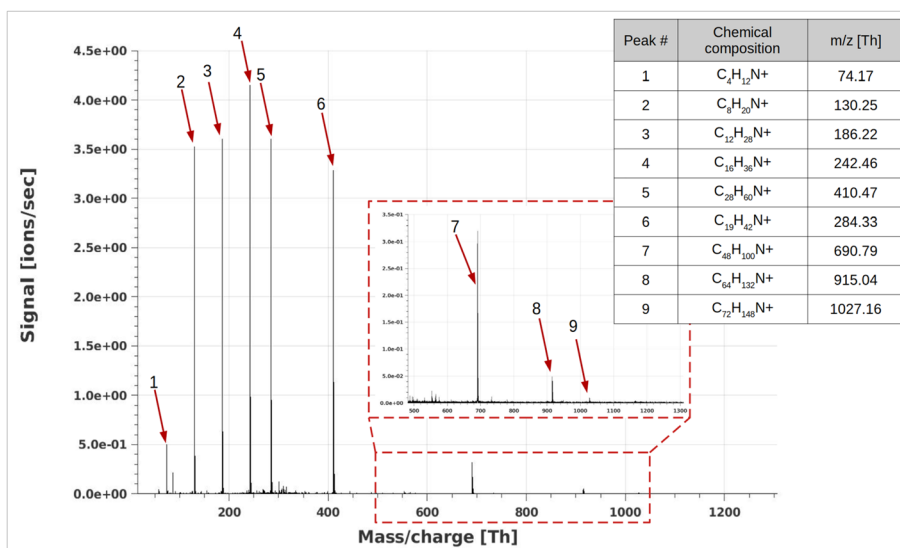


Fig. 2 Mass spectra of the ionic liquid mixture sample measured in positive mode with setup 1. The numbered peaks in the figure are indicated in the table seen in the upper right corner, with chemical composition and  $m/z$  [Th].



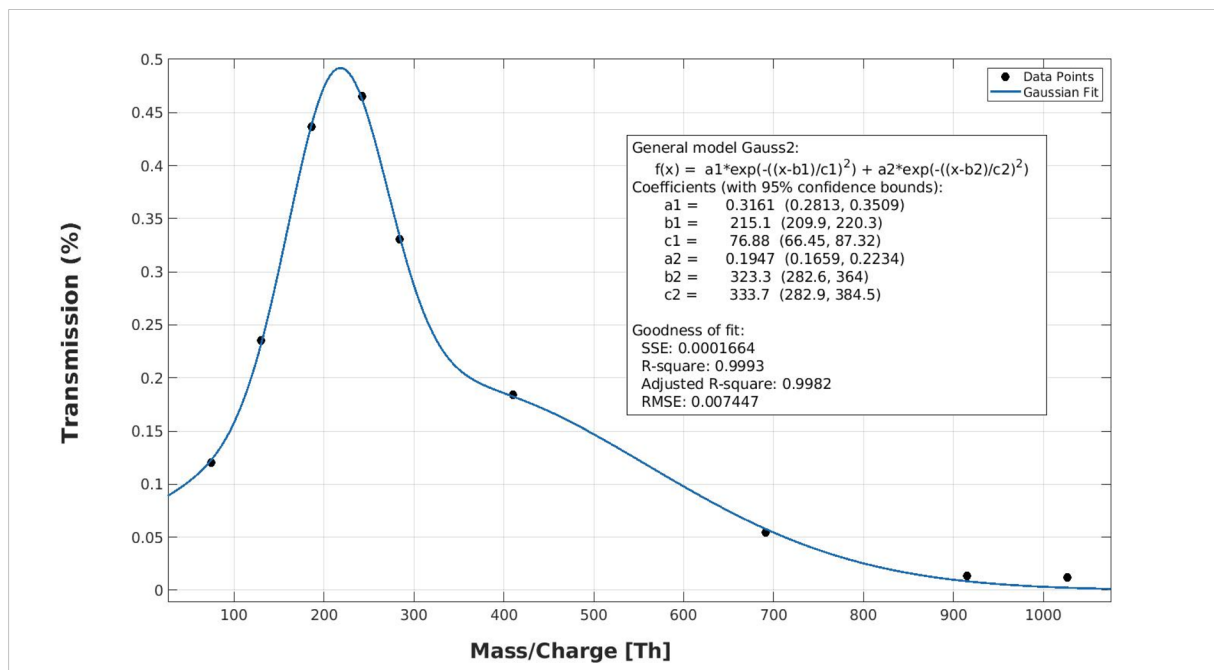


Fig. 3 Transmission [%] versus mass/charge [Th] of the ionic liquid mixture sample, analysis performed in positive mode with setup 1.

A two term Gaussian was fit to the experimental transmission trend. The exact functional form used for the fit was the following:

$$f(x) = a_1 e^{-\left(\frac{x-b_1}{c_1}\right)^2} + a_2 e^{-\left(\frac{x-b_2}{c_2}\right)^2} \quad (1)$$

and the values of the coefficients  $a_1$ ,  $b_1$ ,  $c_1$ ,  $a_2$ ,  $b_2$  and  $c_2$  are reported in the Fig. 3.

The fit yielded an  $R^2$  value of 0.9993. This high  $R^2$  value indicates a strong agreement between the observed data and the fit function, validating the use of the Gaussian function in characterizing the transmission behavior.

**3.1.2 Negative mode.** In the case of negative mode, the primary challenge was identifying a sample as suitable as that used for positive mode analysis. One limitation arose from the nature of the monomers of ionic liquids in negative mode, which consisted solely of bromide ( $\sim 79$  Th) or iodide ions ( $\sim 126$  Th). This restricted their utility compared to positive mode, where nine distinct monomers were available for analysis covering a much broader mass/charge range (up to  $\sim 1027$  Th). We selected a sample sold by Thermo Fisher used to calibrate mass spectrometer. However, the Thermo Fisher sample presented further complications, as its composition was complex, with certain constituents being difficult to identify accurately in terms of chemical composition.

Thermo Fisher provides exact mass/charge values for the primary compounds in their sample, and only these well-characterized, high-confidence peaks were selected and used in this transmission evaluation. Our selected peaks showed mass errors below 5 ppm, consistently matched the expected  $m/z$  values, and exhibited stable signal behavior during fixed-

voltage scans with no or very low interferences from other peaks. Additional unidentified peaks were present in the spectra, neither documented by the manufacturer nor assignable with high confidence based on our analysis, and were therefore excluded from the transmission calculations to avoid introducing uncertainty.

Fig. 4 presents the mass spectra of both the negative samples, highlighting the selected peaks used for transmission evaluation. The selection of peaks was primarily based on their appearance in the fixed-voltage mass spectra. While some peaks showed relatively strong signals in the full mass spectrum, their behavior under fixed-voltage conditions rendered them unsuitable for transmission evaluation.

The transmission percentage, for this measurement, as a function of the mass/charge ratio ( $m/z$ ) is shown in Fig. 5. The transmission in this case started off a bit above 1% for ions in the lower mass range and then exponentially decreased with increasing mass/charge ratio. In Junninen *et al.*, 2010,<sup>4</sup> the only transmission points evaluated in that study were of bromide and their value range between 0.35 and 0.65%. Differences between our values and those of Junninen *et al.* can be attributed to different instrumental settings. Heinritzi *et al.*, 2016,<sup>6</sup> also reported negative mode transmission values using high resolution DMA coupled with an API-ToF MS, and their transmission fit peaked at around 1.5% at mass/charge  $\sim 300$  Th.<sup>4,6</sup>

An exponential function:

$$f(x) = ae^{bx} \quad (2)$$

was used to fit the data points. The values of the coefficients  $a$ , and  $b$  are reported in the Fig. 5. The fit yielded an  $R^2$  value of



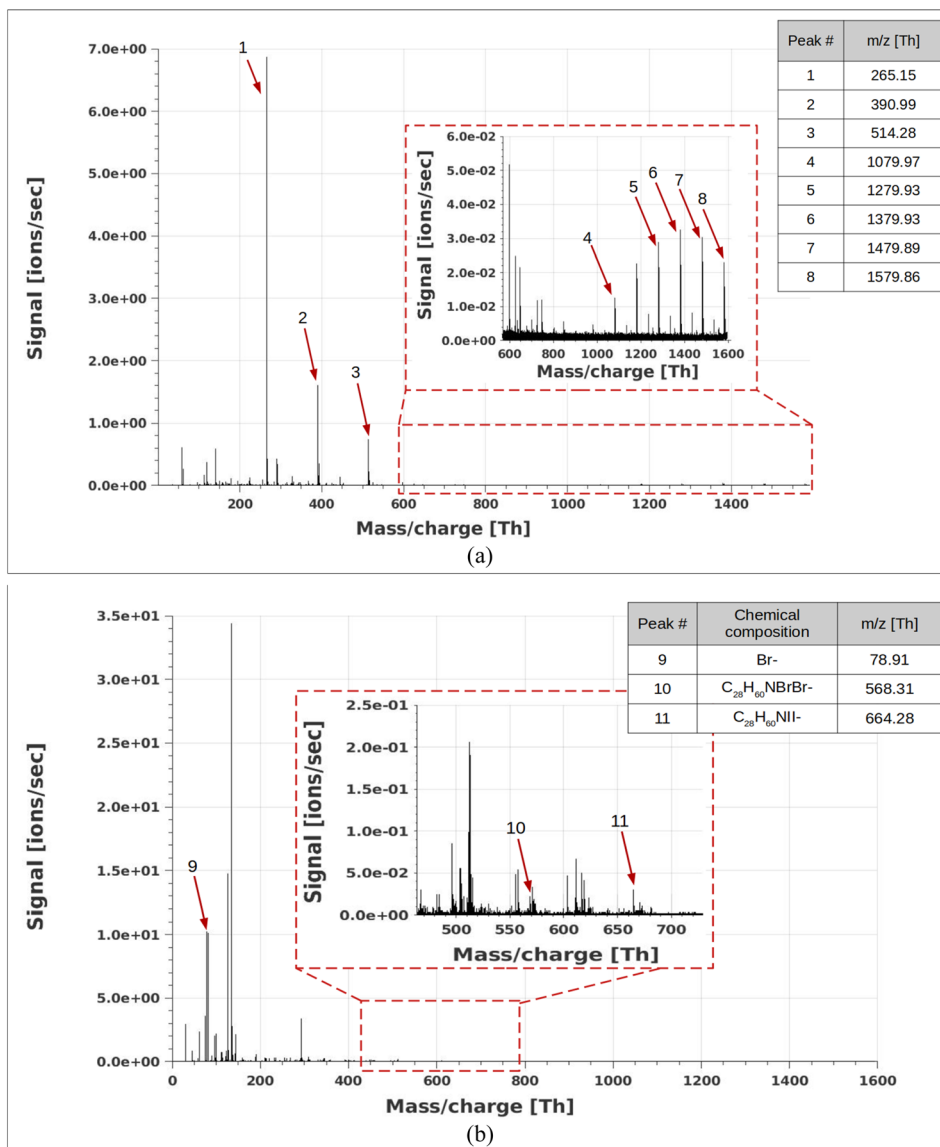


Fig. 4 Mass spectra of (a) the mixture sample from Thermo Fisher and (b) the ionic liquid mixture sample both measured in negative mode with setup 1. The numbered peaks in the figures are indicated in the tables seen in the upper right corners, with their corresponding  $m/z$  [Th].

0.9162, again validating the use of this fit to capture the observed transmission trend.

### 3.2 Setup 2: transmission measurements with wire generator electrospray and Half-mini DMA

An approach to assessing the transmission efficiency of an API-ToF MS involves the use of metal oxide ions generated by a wire-based ion source. This system consists of a metal wire that, when heated by an electric current in a clean airflow, releases metal oxides into the gas phase.<sup>21</sup>

In this study, we performed transmission measurements using a wire generator coupled with a Half-mini Differential Mobility Analyzer (Half-mini DMA). Our initial attempts to integrate the wire generator with a P-DMA, which is primarily designed for use with electrospray ionization, were unsuccessful (most likely due to the high voltage of the front plate).

Consequently, we adapted the experimental setup by employing a DMA (a Half-mini DMA) compatible with the wire generator as an ion source. A key consideration for this experimental setup (setup 2) is that the system with the Half-mini DMA is not directly connected to the API-ToF, as illustrated in Fig. S3 in the SI. The P-DMA is designed for direct coupling with the API-ToF, minimizing ion losses. In contrast, the Half-mini DMA requires a connection to the API-ToF *via* a stainless steel tube, the length and shape of which can vary. This configuration introduces potential ion losses, which must be accounted for when performing transmission measurements. In this study, a 90-degree stainless steel Z-tube was used to connect the outlet of the Half-mini DMA to the inlet of the API-ToF MS, chosen to accommodate the vertical height difference between the two instruments. To address this, we measured the signal intensity both at the outlet of the Half-mini DMA and after the Z-tube



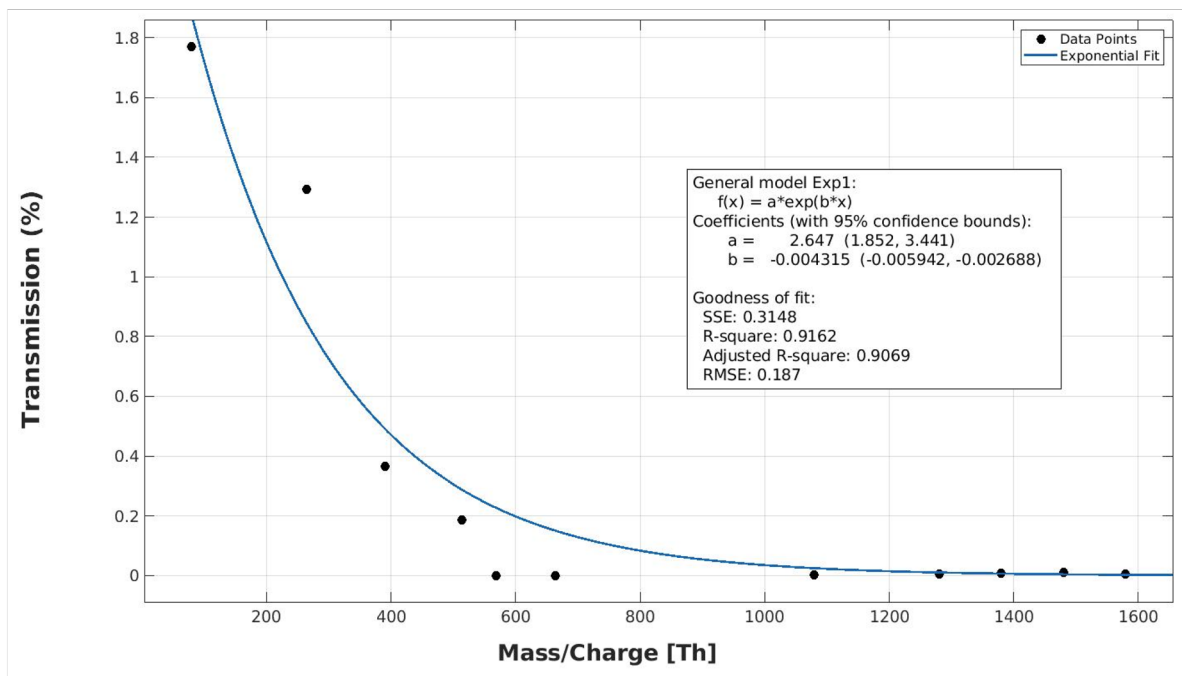


Fig. 5 Transmission [%] versus mass/charge [Th] of the combined ionic liquid and Thermo Fischer samples in negative mode measurements with setup 1.

connection. This comparison enabled us to calculate the extent of signal loss in the tube and apply the necessary corrections to the measured data. Fig. S4 and S5 in the SI illustrate the differences in signal intensity before and after accounting for these losses, along with the calculated signal loss factor.

The experiments were conducted in both positive and negative ionization modes. However, in positive mode, the generation of metal oxide ions resulted in a high number of interference/unknown peaks, preventing accurate and reliable data analysis for constructing a transmission curve. Fig. 3 in Kangasluoma *et al.*, 2016,<sup>22</sup> shows the difference between negative and positive mode peaks generated using a tungsten wire. Despite the use of a different wire (therefore a different metal) in this study, the polarity-dependent trend in spectral complexity of metal oxides formed was similar to that observed in our measurements using the nickel–chromium wire. To our knowledge, the use of a wire generator for positive mode transmission measurements has not been previously documented in published studies. Neither the use of wire generators in negative mode is widely reported; however, it is commonly employed within the community for condensation particle counter (CPC) calibration purposes.

In our experiments we used a nickel–chromium wire to generate chromium oxide and hydroxide ions, as illustrated in Fig. 6. The ions were separated by the DMA and analyzed by MS in negative mode. Similar to Fig. 2, the numbered peaks correspond to the chosen ions presented in the accompanying table within the figure. The mass/charge ( $m/z$ ) range extended up to 616.55 Th in this experiment, approximately 400  $m/z$  lower than the largest peak detected in the ionic liquids sample in the positive mode. Despite the narrower range, the peaks within

this mass region were uniformly distributed, ensuring comprehensive coverage within this range.

Metal oxide and hydroxide ions are generally stable with respect to fragmentation. However, due to the high tendency of the wire generator in conjunction to the Am-charger to charge both the wire itself and any surrounding gases or impurities, the fixed voltage scan measurements for the wire generator appeared considerably more chaotic compared to those of the ionic liquids. Additionally, the metal clusters are produced at high temperature which makes them more prone to collect impurities. This contrast is illustrated in Fig. S6 of the SI, which presents a direct comparison of the mass spectra between the wire generator and the ionic liquids sample under fixed voltage scan conditions. The resulting inaccuracies in transmission calculations for the wire generator measurements stem directly from this issue and span over several hundreds of  $m/z$  Th as seen in the same figure. The problem is further compounded by the resolution differences between the P-DMA and the Half-mini DMA. The P-DMA, with its higher resolution, is capable of better ion separation, leading to cleaner mass spectra with fewer interfering signals.<sup>19</sup> This enhanced resolution allows for more accurate and precise measurements, highlighting the impact of the lower resolution of the Half-mini DMA on the reliability of the transmission data.

For the measurement of the transmission in the case of a single and well-separated ion (for example Fig. S6(b) in SI) the error on the intensity of the signal ( $y$ -axis, transmission %) is very low and it is due to the other peaks present in the spectrum beside the target compound; the error on the  $x$ -axis (mass/charge [Th]) is given by the  $m/z$  range in which the additional peaks are present and their intensity; also in this case the error



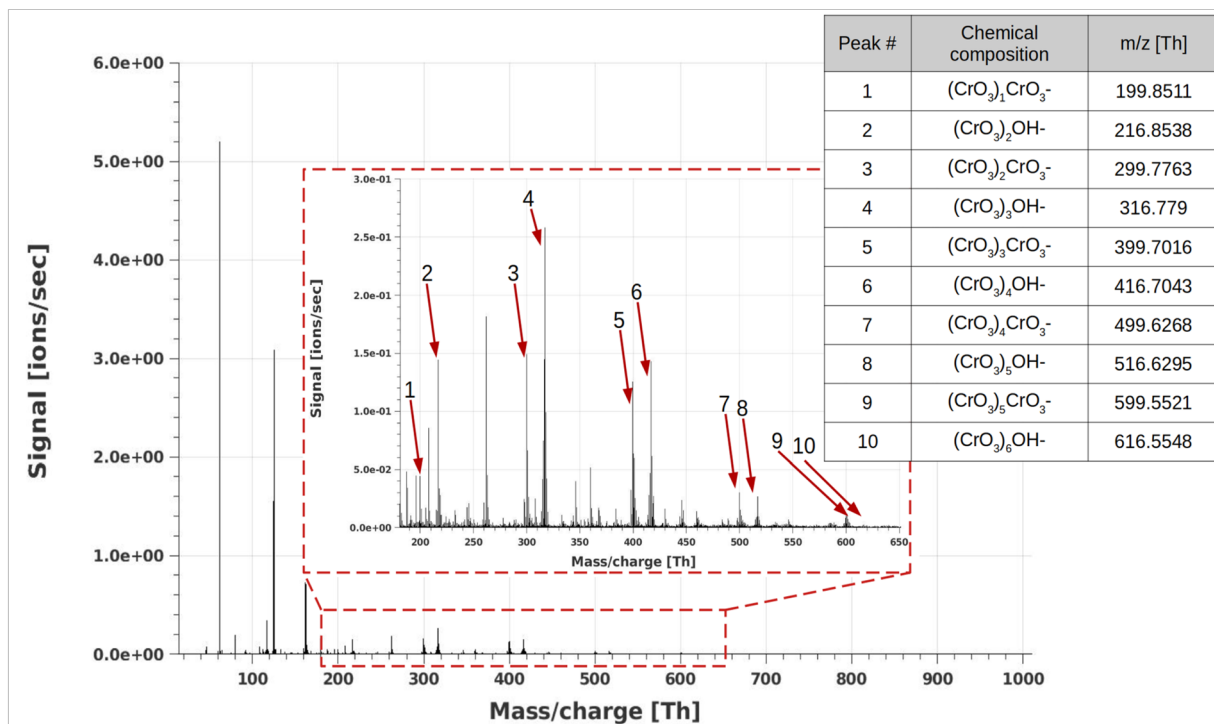


Fig. 6 Mass spectra of the nickel–chromium wire generator, which was employed in negative mode with setup 2. The numbered peaks in the figure are indicated in the table seen in the upper right corner, with their corresponding chemical composition and  $m/z$  [Th].

is negligible. In the case of transmission measurement of several ions not well-separated (for example Fig. S6(a) in SI) there are two approaches to calculate the transmission function. Approach I: it is possible to consider only one selected ion, in this case the error on the  $m/z$  value is low, but there will be a significant underestimation of the transmission (high error on the y-axis) because all the other peaks in the mass spectrum are neglected. This approach was used in the calculation shown in Fig. 7(a), as well as in Fig. S7 in the SI. Another approach (approach II) is to use the sum of the main peaks for determining the transmission percentage. In this way the error on the y-axis decreases; however, there will be a high error on the  $m/z$  value selected for the transmission function (up to several hundreds of Th), leading to the loss of information on the mass-dependence of the transmission. This method was used in the calculation presented in Fig. 7(b). A more detail explanation on the approaches is reported below and in the SI (Paragraph 1).

Fig. 7 shows the calculated transmission percentage across the measured mass range, considering (a) only the selected metal oxide/hydroxide peak intensity and (b) the total intensities of all identifiable peaks present in the mass spectrum of the corresponding fixed voltage scan runs. The transmission efficiency in Fig. 7(a) peaked at approximately 0.025% for intermediate mass ranges, exhibiting a similar decline in transmission for both lower and higher masses, as observed in the ionic liquids measurements. The data was fitted using a Gaussian model similar to the one applied to the ionic liquids, but utilizing a single-term fit in this case. The  $R^2$  value for this fit was 0.8531. The functional used for the fit was as follows:

$$f(x) = a_1 e^{\left(-\left(\frac{x-b_1}{c_1}\right)^2\right)} \quad (3)$$

and the values of the coefficients  $a_1$ ,  $b_1$  and  $c_1$  are reported in the Fig. 7(a).

Fig. 7(b) shows that the maximum transmission efficiency exceeds 0.3%, which is much closer than that in Fig. 7(a) to the values measured in negative mode with our combined samples using the ESI-P-DMA-APi-ToF MS setup. The fit function used is an exponential (eqn (2)) and the values of the coefficients  $a$ , and  $b$  are reported in the Fig. 7(b). The choice between the use of approach I or II strongly depends on the data. The general rule is that the approach I is preferred when the fix-voltage scan mass spectra are clean (only few peaks and a main one with high intensity) as shown in Fig. S6b (in SI); approach II is preferred when the number and the intensity of peaks in the fix-voltage mass spectra is increasing (an example is reported in Fig. S6a in the SI). In our case, due to the elevate number and intensity of the peaks in the fix-voltages scan mass spectra the best approach is II, otherwise the underestimation of the transmission is too high (more than one order of magnitude).

For comparison, Fig. S7 presents a transmission plot generated using the same setup in 2016 by Monica Passananti and reported in Alfaouri *et al.*, 2022.<sup>15</sup> Both plots (Fig. S7 and 7(a)) exhibit a similar peak in transmission, though the 2016 data was fitted with a third-degree polynomial, yielding an  $R^2$  value of 0.9422, which indicates a slightly better fit for that data set ( $R^2$  value for this papers transmission measurement using a third-degree polynomial fit would yield a value of 0.8454).



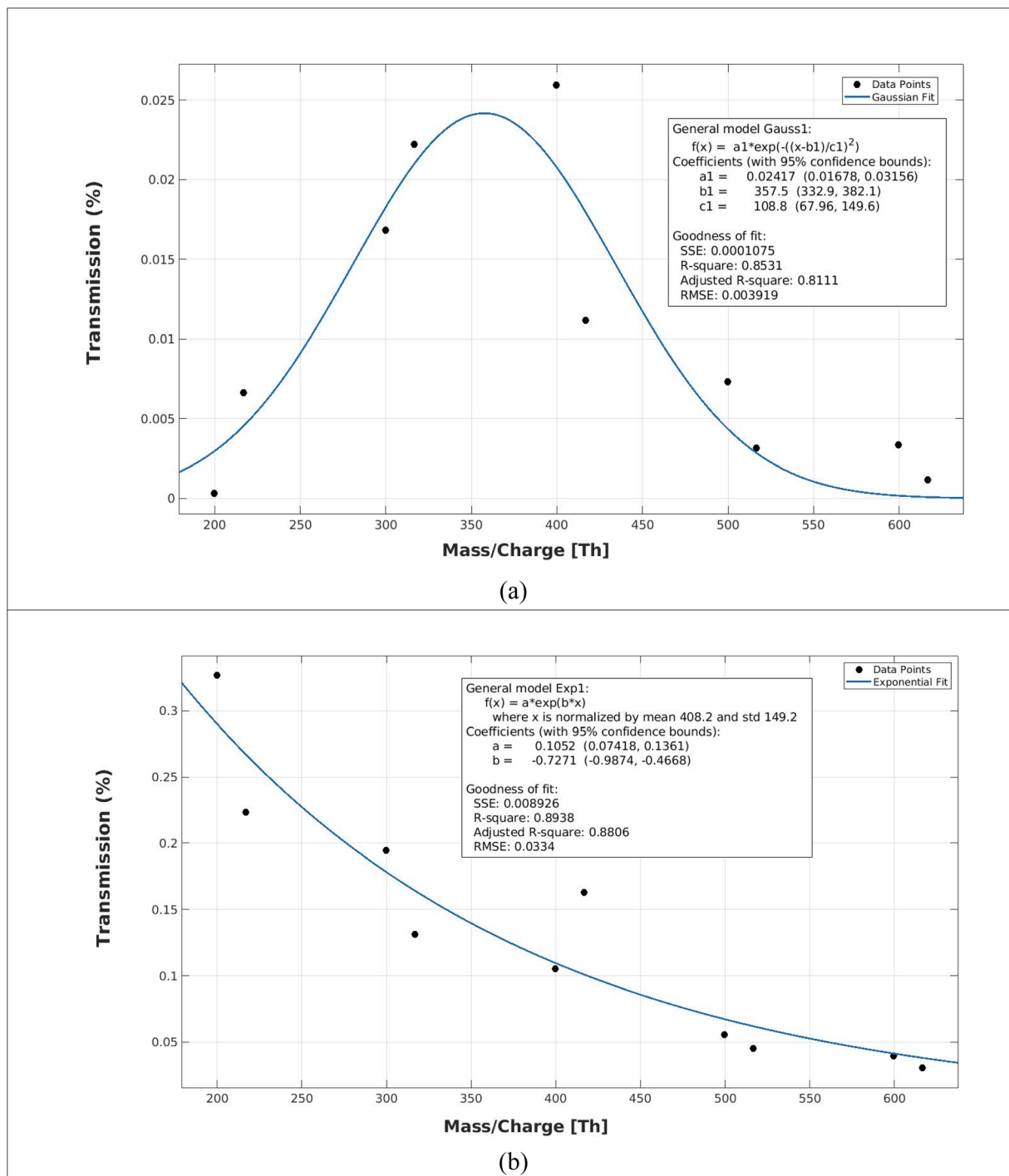


Fig. 7 Transmission [%] versus mass/charge [Th] of the nickel–chromium wire generator measurements in negative mode for (a) just solely the metal oxide/hydroxide peak of interest, and (b) for the total signal of all identifiable peaks appearing in the MS of the fixed voltage scans.

Despite the different fitting models, the similarity in peak transmission values between the 2016 and 2024 measurements suggests minimal decline in the instrument's performance over this period. This consistency reflects the reliability and stability of the setup over several years.

### 3.3 Comparison between different transmission functions

In our experiments, we observed differences in both the shape and magnitude of the transmission curves that could be mainly attribute to instrument's characteristics, voltage configuration and polarity. In general, the transmission of ions inside a mass spectrometer depends on several factors, such as the voltages configuration, the geometry, and the pressure inside the



instrument. As shown in literature,<sup>4,6</sup> ion transmission can vary by orders of magnitude depending on voltage configuration parameters such as RF amplitude, ion funnel voltage, and skimmer bias. These factors could lead to different transmission curves, that will be described by different functions. To select an appropriate fitting function for each case, we applied a three-tiered evaluation:

- (1) Goodness of fit to the experimental data, assessed *via*  $R^2$  values (typically between 0.85 and 0.98),
- (2) Visual consistency with the overall trend across the full measured mass/charge range, and
- (3) Physical plausibility of the extrapolation beyond the measured data, particularly at high mass/charge, where some functions can produce nonphysical results such as negative transmission or unrealistic increases.

This selection strategy ensures that the fitting functions not only represent the data as accurately as possible but also behave reasonably outside the measurement range.

We observed distinct transmission trends for positive and negative ion modes. In positive mode, transmission was generally enhanced for intermediate mass/charge values (200–500 Th), whereas in negative mode, higher transmission was observed for smaller ions (<300 Th). These trends reflect the fact that the API-ToF MS uses separate, polarity-specific voltage configurations, which were independently optimized in our lab for signal stability and ion focusing. This difference could be explained by a combination of factors. Indeed, the transmission depends strongly on the RF voltage applied to the two quadrupoles present in the first two API chambers, but it is also influenced by the ion beam's shape as it enters the quadrupole. Increased beam divergence shifts the transmission peak toward lower  $m/z$  values, intensifying the loss of heavier ions, whereas off-axis beam profiles have a counteracting effect. In practical applications, the exact profile depends on tuning parameters and beam alignment precision. Also, the orthogonal extraction unit of the TOF can have an impact on the ion transmission, as well as the multi-channel plate (MCP) detector used in TOF systems can introduce mass-dependent detection biases.<sup>23–25</sup> The specific configurations used in this study are provided in Fig. S8 and S9 of the SI.

It is important to emphasize that voltage tuning has a substantial impact on transmission efficiency, consistent with previous findings in the literature. Therefore, transmission should ideally be re-characterized whenever the voltage settings are modified for different applications, such as optimizing for low mass/charge detection or maximizing sensitivity.

As shown in Fig. 5 and 7(a), there is a difference of about 70-fold between the maximum transmission values for the same measured mode and instrumental settings. This discrepancy is primarily due to the inaccuracies discussed earlier when using the wire generator. A more accurate result is obtained when the transmission efficiency is calculated using the total signal of all identifiable wire generator peaks, as shown in Fig. 7(b). To account for the total MS signal at each fixed voltage scan, including all detected peaks, whether secondary ions or impurities would even increase the transmission percentage, but increasing also the error on the  $m/z$  values. This led to an

increase in the intensity of the measured transmission; however, it can induce an error in the type of function describing the transmission curve due to the high error on the  $x$ -axis. Indeed, the fitting curve changes from Gaussian (Fig. 7(a)) to exponential (Fig. 7(b)). These results highlight the importance of accurate transmission measurement to avoid significant errors in defining the transmission function curves.

To improve the transmission measurements, another approach would be to utilize a higher-resolution DMA, capable of better separating ions with close mobilities. Nevertheless, this approach will not completely solve the problem because the wire generator (coupled with the Am-charger) produces a large variety of metal clusters (oxides, nitrates, hydroxides, *etc.*) which are difficult to separate even with a high-resolution DMA. We attempted this approach in the current study, but the effort was unsuccessful with the current P-DMA configuration.

## 4. Conclusion

In this study, we examined the performance and transmission characteristics of an atmospheric pressure interface time-of-flight mass spectrometer (API-ToF MS) coupled with two different ion sources, including electrospray ionization (ESI) and a nickel–chromium wire generator. The aim of the work was to compare different methods and identify the best procedure to accurately measure the transmission of an API-ToF MS. The results revealed distinct transmission efficiency trends across different mass ranges for both positive and negative ion modes. In general, transmission efficiency peaked at intermediate mass ranges, with a clear decline observed at both lower and higher masses for positive mode, while for negative mode the transmission exhibited more of an exponential decrease with higher masses. These transmission patterns, which were captured using Gaussian and exponential fits, provided insights into the instrument's performance and its mass-dependent transmission behavior.

A direct comparison of fixed voltage scan measurements between the ionic liquids and the chromium oxide/hydroxide ions from the wire generator showed more chaotic mass spectra for the latter. This is primarily due to the increased tendency of both the wire generator and the Am-charger to ionize surrounding gases and impurities, along with the lower resolving power of the Half-mini DMA. This behavior inherently affected the accuracy of transmission calculations using chromium oxide/hydroxide ions. We have shown that the wire generator coupled with a DMA, may lead to significant error in the evaluation of the transmission. A few points need to be considered both during the data analysis and the lab experiments for improving the transmission measurement. For example, since the DMA (in our experiment a Half-mini DMA) is usually not directly connected to the API-ToF MS, extra experiments are required to calculate ion losses in the tubing. Overall, we showed that the ESI–P-DMA–API-ToF MS setup proved to be significantly more reliable, accurate, and user-friendly than the wire generator–Half-mini DMA–API-ToF MS configuration.

Furthermore, a comparison of transmission data from 2016 and 2024 using the same experimental setup (Fig. 1(b)) showed



that the instrument's performance has remained consistent over time, with minimal deterioration in transmission values. Despite the use of different fitting functions, the similarity in peak transmission values across the two years confirms the long-term stability and reliability of the setup. Further studies could focus on a comprehensive investigation across various instrumental settings (including the duty cycle of the ToF) that influence the transmission to define the key parameters that could be adjusted to optimize the transmission of an API-ToF MS.

Overall, our results provide critical insights into the instrument's performance, particularly in terms of its mass-dependent transmission efficiency, which is crucial for interpreting and quantifying experimental measurements accurately. Finally, a direct comparison between the two measurement methods for the same mode (negative mode) showed the possible inaccuracies resulting from the use of the wire generator for transmission efficiency evaluation. These results highlighted the importance of defining simple and reliable procedures to characterize the API-ToF MS, in particular the transmission function, to calculate the concentration of reactive gases and condensable vapors with a good accuracy.

## Conflicts of interest

There are no conflicts to declare.

## Data availability

Data for this article are available at GitHub at <https://github.com/DinaAlfaouri/An-optimization-of-transmission-measurement-of-an-API-ToF-MS.git>. Moreover, additional data supporting this article have been included as part of the supplementary information (SI). Supplementary information: the figures of mass spectra of fixed scans, the electrometer signals and pictures of the used experimental setups, the signal loss factor figure, transmission curve reported previously for the same setup, the voltage settings of the MS in both polarities and finally a text about the errors from different approaches used to calculate the transmission. See DOI: <https://doi.org/10.1039/d5ea00029g>.

## Acknowledgements

We thank the ERC Projects 692891-DAMOCLES, and 948666-ERC-2020-StG NaPuE, Academy of Finland, and the University of Helsinki for funding. We also thank Yiliang Liu, Rima Baalbaki and Sebastian Holm for their help in assembling and testing one of the setups used in this study. We acknowledge ACTRIS CiGas – Centre for Reactive Trace Gases *In Situ* Measurements for providing support.

## References

1 M. Kulmala, T. Petäjä, M. Ehn, J. Thornton, M. Sipilä, D. R. Worsnop and V.-M. Kerminen, Chemistry of Atmospheric Nucleation: On the Recent Advances on

Precursor Characterization and Atmospheric Cluster Composition in Connection with Atmospheric New Particle Formation, *Annu. Rev. Phys. Chem.*, 2014, **65**, 21–37.

- W. Zhang, L. Xu and H. Zhang, Recent advances in mass spectrometry techniques for atmospheric chemistry research on molecular-level, *Mass Spectrom. Rev.*, 2024, **43**, 1091–1134.
- C. M. Fisher, K. T. Peter, S. R. Newton, A. J. Schaub and J. R. Sobus, Approaches for assessing performance of high-resolution mass spectrometry-based non-targeted analysis methods, *Anal. Bioanal. Chem.*, 2022, **414**, 6455–6471.
- H. Junninen, M. Ehn, T. Petäjä, L. Luosujärvi, T. Kotiaho, R. Kostianinen, U. Rohner, M. Gonin, K. Fuhrer, M. Kulmala and D. R. Worsnop, A high-resolution mass spectrometer to measure atmospheric ion composition, *Atmos. Meas. Tech.*, 2010, **3**, 1039–1053.
- T. Olenius, S. Schobesberger, O. Kupiainen-Määttä, A. Franchin, H. Junninen, I. K. Ortega, T. Kurtén, V. Loukonen, D. R. Worsnop, M. Kulmala and H. Vehkamäki, Comparing simulated and experimental molecular cluster distributions, *Faraday Discuss.*, 2013, **165**, 75.
- M. Heinritzi, M. Simon, G. Steiner, A. C. Wagner, A. Kürten, A. Hansel and J. Curtius, Characterization of the mass-dependent transmission efficiency of a CIMS, *Atmos. Meas. Tech.*, 2016, **9**, 1449–1460.
- M. Passananti, E. Zapadinsky, T. Zanca, J. Kangasluoma, N. Myllys, M. P. Rissanen, T. Kurtén, M. Ehn, M. Attoui and H. Vehkamäki, How well can we predict cluster fragmentation inside a mass spectrometer?, *Chem. Commun.*, 2019, **55**, 5946–5949.
- T. Jokinen, K. Lehtipalo, R. C. Thakur, I. Ylivinkka, K. Neitola, N. Sarnela, T. Laitinen, M. Kulmala, T. Petäjä and M. Sipilä, Measurement report: Long-term measurements of aerosol precursor concentrations in the Finnish subarctic boreal forest, *Atmos. Chem. Phys.*, 2022, **22**, 2237–2254.
- M. Riva, P. Rantala, J. E. Krechmer, O. Peräkylä, Y. Zhang, L. Heikkinen, O. Garmash, C. Yan, M. Kulmala, D. Worsnop and M. Ehn, Evaluating the performance of five different chemical ionization techniques for detecting gaseous oxygenated organic species, *Atmos. Meas. Tech.*, 2019, **12**, 2403–2421.
- A. Kürten, L. Rondo, S. Ehrhart and J. Curtius, Calibration of a Chemical Ionization Mass Spectrometer for the Measurement of Gaseous Sulfuric Acid, *J. Phys. Chem. A*, 2012, **116**, 6375–6386.
- M. Ehn, J. A. Thornton, E. Kleist, M. Sipilä, H. Junninen, I. Pullinen, M. Springer, F. Rubach, R. Tillmann, B. Lee, F. Lopez-Hilfiker, S. Andres, I.-H. Acir, M. Rissanen, T. Jokinen, S. Schobesberger, J. Kangasluoma, J. Kontkanen, T. Nieminen, T. Kurtén, L. B. Nielsen, S. Jørgensen, H. G. Kjaergaard, M. Canagaratna, M. D. Maso, T. Berndt, T. Petäjä, A. Wahner, V.-M. Kerminen, M. Kulmala, D. R. Worsnop, J. Wildt and T. F. Mentel, A large source of low-volatility secondary organic aerosol, *Nature*, 2014, **506**, 476–479.



- 12 G. Sharma, M. Wang, M. Attoui, X. You and P. Biswas, Measurement of sub-3 nm flame-generated particles using butanol CPCs in boosted conditions, *Aerosol Sci. Technol.*, 2021, **55**, 785–794.
- 13 S. V. Hering, G. S. Lewis, S. R. Spielman, A. Eiguren-Fernandez, N. M. Kreisberg, C. Kuang and M. Attoui, Detection near 1-nm with a laminar-flow, water-based condensation particle counter, *Aerosol Sci. Technol.*, 2017, **51**, 354–362.
- 14 T. Jokinen, M. Sipilä, H. Junninen, M. Ehn, G. Lönn, J. Hakala, T. Petäjä, R. L. Mauldin, M. Kulmala and D. R. Worsnop, Atmospheric sulphuric acid and neutral cluster measurements using CI-API-TOF, *Atmos. Chem. Phys.*, 2012, **12**, 4117–4125.
- 15 D. Alfaouri, M. Passananti, T. Zanca, L. Ahonen, J. Kangasluoma, J. Kubečka, N. Myllys and H. Vehkamäki, A study on the fragmentation of sulfuric acid and dimethylamine clusters inside an atmospheric pressure interface time-of-flight mass spectrometer, *Atmos. Meas. Tech.*, 2022, **15**, 11–19.
- 16 R. Cai, D. Yang, L. R. Ahonen, L. Shi, F. Korhonen, Y. Ma, J. Hao, T. Petäjä, J. Zheng, J. Kangasluoma and J. Jiang, Data inversion methods to determine sub-3 nm aerosol size distributions using the particle size magnifier, *Atmos. Meas. Tech.*, 2018, **11**, 4477–4491.
- 17 J. Fernández de la Mora and J. Kozlowski, Hand-held differential mobility analyzers of high resolution for 1–30 nm particles: Design and fabrication considerations, *J. Aerosol Sci.*, 2013, **57**, 45–53.
- 18 L. A. Doezema, T. Longin, W. Cody, V. Perraud, M. L. Dawson, M. J. Ezell, J. Greaves, K. R. Johnson and B. J. Finlayson-Pitts, Analysis of secondary organic aerosols in air using extractive electrospray ionization mass spectrometry (EESI-MS), *RSC Adv.*, 2012, **2**, 2930.
- 19 M. Amo-González and S. Pérez, Planar Differential Mobility Analyzer with a Resolving Power of 110, *Anal. Chem.*, 2018, **90**, 6735–6741.
- 20 A. Bianco, I. Neeffjes, D. Alfaouri, H. Vehkamäki, T. Kurtén, L. Ahonen, M. Passananti and J. Kangasluoma, Separation of isomers using a differential mobility analyser (DMA): Comparison of experimental vs. modelled ion mobility, *Talanta*, 2022, **243**, 123339.
- 21 M. Attoui, Mobility distributions of Sub 5 nm singly self-charged water soluble and non-soluble particles from a heated NiCr wire in clean dry air, *Aerosol Sci. Technol.*, 2022, **56**, 859–868.
- 22 J. Kangasluoma, A. Samodurov, M. Attoui, A. Franchin, H. Junninen, F. Korhonen, T. Kurtén, H. Vehkamäki, M. Sipilä, K. Lehtipalo, D. R. Worsnop, T. Petäjä and M. Kulmala, Heterogeneous Nucleation onto Ions and Neutralized Ions: Insights into Sign-Preference, *J. Phys. Chem. C*, 2016, **120**, 7444–7450.
- 23 I. V. Chernushevich, A. V. Loboda and B. A. Thomson, An introduction to quadrupole–time-of-flight mass spectrometry, *J. Mass Spectrom.*, 2001, **36**, 849–865.
- 24 M. Müller, T. Mikoviny, S. Feil, S. Haidacher, G. Hanel, E. Hartungen, A. Jordan, L. Märk, P. Mutschlechner, R. Schottkowsky, P. Sulzer, J. H. Crawford and A. Wisthaler, A compact PTR-ToF-MS instrument for airborne measurements of volatile organic compounds at high spatiotemporal resolution, *Atmos. Meas. Tech.*, 2014, **7**, 3763–3772.
- 25 F. Muntean, D. Ursu and N. Lupsa, Ion trajectory analysis for rf-only quadrupoles, *Vacuum*, 1995, **46**, 131–137.

